2007

Baroclinic Effects and Tides on the Cape Hatteras Continental Shelf

Dana K. Savidge

Catherine R. Edwards

Mark Santana
Old Dominion University

Original Publication Citation

Savidge, D. K., Edwards, C. R., & Santana, M. (2007). Baroclinic effects and tides on the Cape Hatteras continental shelf. *Journal of Geophysical Research: Oceans, 112*(C9), C09016. doi:10.1029/2006jc003832

Baroclinic effects and tides on the Cape Hatteras continental shelf

Dana K. Savidge,[1] Catherine R. Edwards,[2] and Mark Santana[3]

Received 22 July 2006; revised 25 May 2007; accepted 14 June 2007; published 20 September 2007.

[1] Seasonal variability has been identified on the shelf near Cape Hatteras in the semidiurnal and diurnal frequency bands. Large summertime semidiurnal currents appear to be an M2 internal tide whose propagation shoreward is supported by strong Middle Atlantic Bight (MAB) seasonal stratification. At the southern limit of the MAB, strong MAB stratification gives way to weaker seasonal stratification in the South Atlantic Bight (SAB), and the M2 internal tide propagates shoreward less effectively. Strong diurnal variability appears in K1 and O1 components in summer, achieving magnitudes as large as the M2. The diurnal components are typically much smaller than M2 in winter. However, this summer signal is unlikely to be a diurnal internal tide since at these latitudes (34.5–36.5N) the diurnal frequency is subinertial. Coastally trapped waves (CTWs) are presented as a mechanism to explain the increased variability in the diurnal band under summertime stratification. Alongshore southward propagation of the diurnal variability is evident from moorings on the middle and outer shelf (phase speed of 2.1–2.6 m/s along the 60-m isobath) as far south as Cape Hatteras, but little energy in this band propagates past Cape Hatteras. While diurnal band CTW propagation will not occur at this latitude under well-mixed conditions, stratification could cause those frequencies to become available for a given wave number, as described in the work of Brink (1990). Estimates of the Huthnance (1978) stratification and slope parameter A, and the Burger number S, suggest the summertime diurnal signal is consistent with baroclinic CTWs. If so, these are the first observations of diurnal CTWs at Cape Hatteras.

Citation: Savidge, D. K., C. R. Edwards, and M. Santana (2007), Baroclinic effects and tides on the Cape Hatteras continental shelf, *J. Geophys. Res.*, *112*, C09016, doi:10.1029/2006JC003832.

1. Introduction and Background

[2] Tides on the shelf near Cape Hatteras have been examined in the past based on one- to several-month time series from current meter and pressure gauge moorings [*Pietrafesa et al.*, 1985; *Lentz et al.*, 2001], focusing exclusively on the barotropic tide. Barotropic tidal currents are dominated by the M2 semidiurnal constituent, and are typically of fairly small magnitude (of order 10 cm/s or less), relative to subtidal velocities due to Gulf Stream, wind, and buoyancy forcing, which can exceed several tens of cm/s in 40-hour low-passed (HLP) data [*Savidge*, 2002, 2004]. However, on short timescales (up to a few months), the tide can account for up to 50% of the variability.

[3] Baroclinic tides may also be important at specific sites intermittently, since the Cape Hatteras region exhibits strong and variable vertical stratification year-round. Additionally, horizontal stratification may be an important control on baroclinic tide propagation on the shelf, owing to the presence of several strong mesoscale fronts, shown schematically (Figure 1), and discussed in section 3. These fronts and frontally derived features are not stationary on the shelf, but can migrate under wind and Gulf Stream forcing. The combination of the strong summertime vertical stratification and the presence of these horizontal fronts can potentially support a variety of internal tides, while the spatial and temporal variability of the stratification may alter the internal tide as it propagates.

[4] *FRED Group* [1989] observed M2 internal tides off of Cape Fear, the second Cape southwest of Cape Hatteras (~250 km to the southwest), but did not detect them between Cape Fear and Cape Hatteras. They speculated that the characteristic slope [*Baines*, 1982] of the M2 internal tide would be too small in this region to allow propagation up the bathymetric slope, and concluded that internal tides would not be generated north of their observations at Cape Fear. Offshore of Virginia, ~160 km north of Cape Hatteras, *Nash et al.* [2004] observed enhanced near-bottom mixing seaward of the slope, which they associated with the reflection of the M2 internal tide near the 1000-m isobath of the continental slope. Their results suggested weak M2 reflection at the shelf break, consistent with the supercritical slope and with the modeling results of *Legg* [2004] for barotropic forcing. However, strong shelf

[1] Skidaway Institute of Oceanography, Savannah, Georgia, USA.
[2] Department of Marine Sciences, University of North Carolina, Chapel Hill, North Carolina, USA.
[3] Center for Coastal Physical Oceanography, Old Dominion University, Norfolk, Virginia, USA.

0148-0227/07/2006JC003832

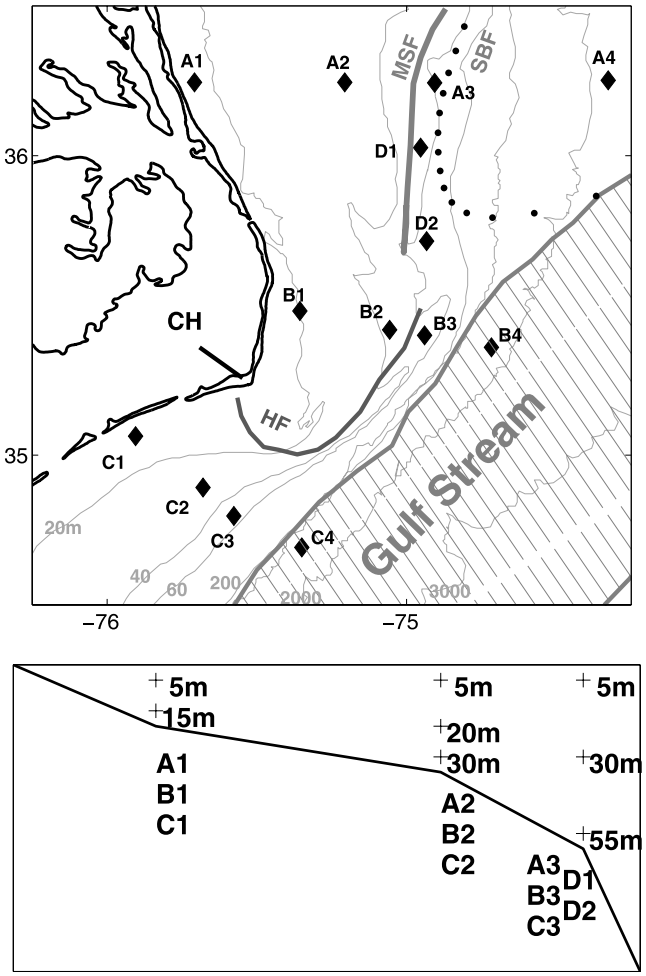

Figure 1. (top) Map of the study region near Cape Hatteras, North Carolina (CH). Schematic Hatteras Front (HF), Gulf Stream and Mid Shelf Front (MSF) are shown. The Shelf-Break Front (SBF) location is shown by Georges Bank GLOBEC drifter track (dots at daily intervals along the 200-m isobath in the northwest corner of the map; data courtesy of Glen Gawarkiewicz). (bottom) Schematic mooring line design. Shelf moorings were situated at the 20-, 35-, and 60-m isobaths, with slope moorings at the 2000- and 3000-m isobaths. Shelf mooring numbers increment from 1 to 3 in the seaward direction. Shelf and shelf-edge moorings had 2–3 instrument packages in the vertical, including InterOcean S4 and General Oceanic MkII winged current meters, with temperature and salinity sensors.

internal tides have been observed shoreward of supercritical slope regions [*Lerczak et al.*, 2003; *Holloway et al.*, 2001], as barotropic tidal flow across critical portions of the upper slope may generate an internal tide that can propagate onshore.

[5] In the following, it is shown that strong increases in energy at semidiurnal and diurnal frequencies appear seasonally on the Hatteras shelf. Strong spatial variability is also evident, apparently associated with strong spatial gradients in density. Largest signals appear at the shelf break during summer, coincident with periods of strongest stratification. The seasonal variability in the semidiurnal is attributed to an internal M2 tide. Seasonal variability in the diurnal may not be an internal tide: at these latitudes, the diurnal internal tide is subinertial and cannot freely propagate at K1 or O1 frequencies through the region without a source of significant anticyclonic shear (1–2 m/s over 50 km). The likely mechanisms for seasonal variability at near-diurnal frequencies seem to be either a forced/trapped internal tide or a subtidal mechanism such as coastally trapped waves propagating at the diurnal. These possibilities are explored in section 5.

2. Data and Methods

[6] The data used in this study were collected by a multi-institutional team funded by the Minerals Management Service (MMS) [*Berger et al.*, 1995]. During the MMS project, eleven shelf and shelf-edge mooring locations were occupied continuously for a two-year span, from March 1992 through February 1994 (Figure 1). These moorings bracketed Cape Hatteras with three cross-shelf lines, the A, B, and C lines, and one alongshelf pair of moorings, the D line (Figure 1). On each of the cross-shelf lines, there were shallow moorings at the 20-, 35-, and 60-m isobaths, each with current meters at two or three depths in the vertical. Several additional moorings on the 2000- and 3000-m isobaths will not be discussed. Currents on the shelf were measured with InterOcean S4 and General Oceanic MkII winged current meters, with S4s at 5 and 14.3 m at the 20-m isobath stations, and also at 5-m depth on the 35- and 60-m isobath stations (Figure 1). Raw data were 3-hour low-pass (3-HLP) filtered with a Lanczos kernel and subsampled to hourly values.

[7] For density, wind, and subtidal analysis presented in section 3, current meter, wind, and temperature data were processed with a 48-HLP Hanning filter and subsampled to daily noon values. These low-passed records are used primarily to describe the spatial and temporal variation of the density field that internal tides may encounter on the shelf. Wind data are from the National Data Buoy Center Coastal Marine Automated Network (C-MAN). The primary record is DSLN7, off Cape Hatteras over Diamond Shoals. Short gaps in this record were filled with CLKN7 winds, off Cape Lookout south of Cape Hatteras, with means and standard deviations adjusted to match those at DSLN7.

[8] The tidal analyses in sections 4 and 5 are derived from the high-resolution (hourly or half-hourly) 3-HLP current meter data. These data were harmonically analyzed in running three-month subsections, stepping in one-month intervals, using the T_tide software developed by Pawlowicz, based on the Foreman tidal analysis software [*Pawlowicz et al.*, 2002; *Godin*, 1972; *Foreman*, 1977, 1978]. No bottom pressure data were collected on the shelf during the MMS-sponsored experiment, so the results and discussion below apply only to tidal currents, and not variations in sea-surface height. The vertical variability in the tide has been examined here by tidal analysis on total variability at each record in the vertical. Since a phase lag exists from bottom to top in the tidal constituents of interest (M2, K1, O1) at many locations, a depth mean representation of tidal variability was not removed. Where the bottom boundary layer occu-

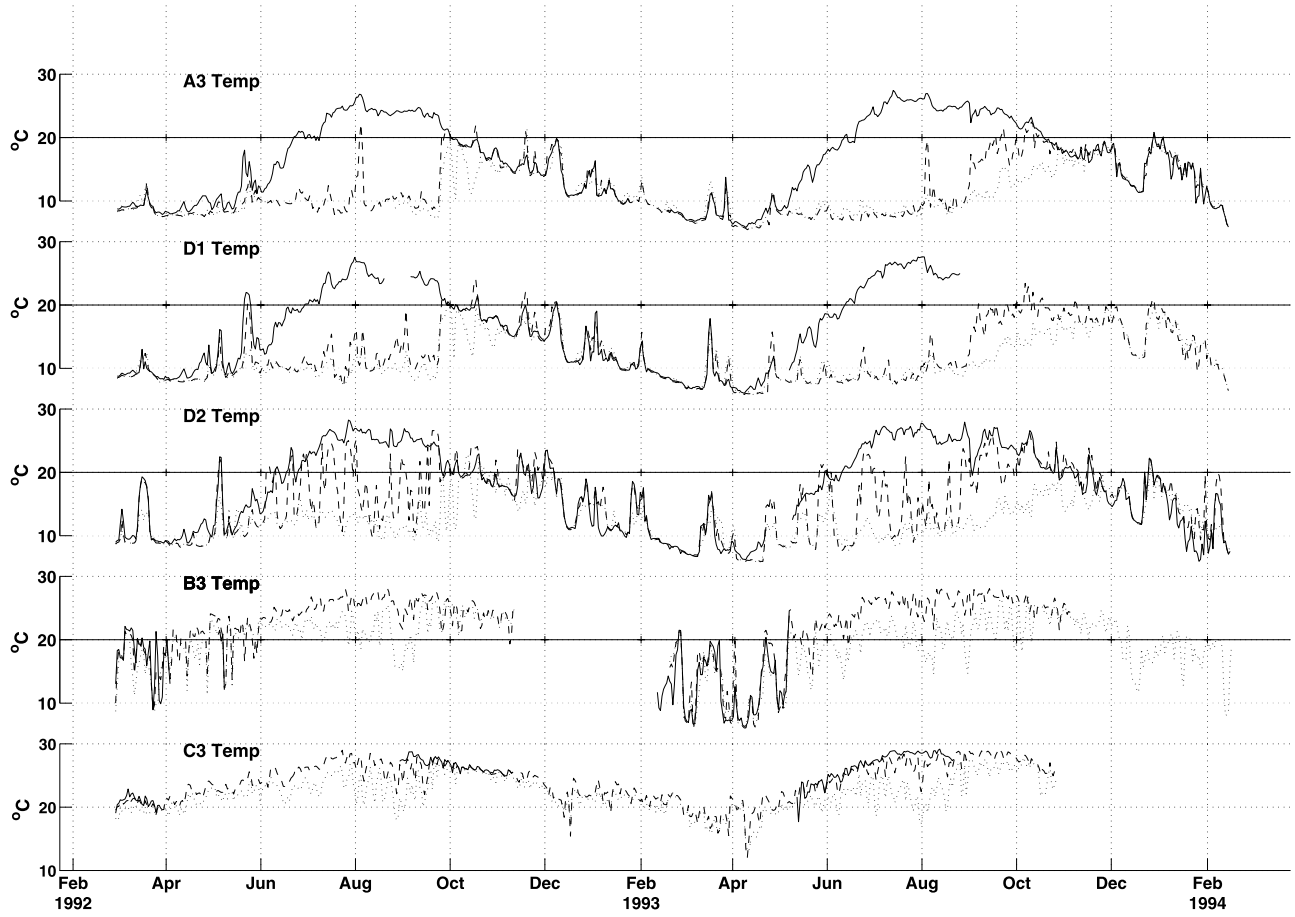

Figure 2. Temperature records (48HLP) from shelf-edge (60-m isobath) moorings. Near-surface (solid line), middepth (dashed line), and near bottom (dotted line) are shown in each panel. Five panels are arranged top to bottom to represent relative mooring locations, north to south.

pies a significant fraction of the water column, depth averaging can introduce the frictional shear associated with the barotropic tide into the estimate of ''baroclinic'' motions. EOF analysis to separate barotropic and baroclinic velocity structures is an improvement to depth averaging in shallow water [*Edwards and Seim*, 2007], but the degrees of freedom provided by the limited vertical coverage in this data set are insufficient for application to the MMS current meter data.

[9] The tidal database of *Blanton et al.* [2004], computed using the Advanced Circulation (ADCIRC) model for oceanic, coastal, and estuarine waters of the Western North Atlantic [*Luettich et al.*, 1992], is used to set the temporal and spatial variability of the three-month running tidal fits to the data into the context of larger spatial patterns of the barotropic tide. Velocity data from the 1996 Ocean Margins Project (OMP) [*Verity et al.*, 2002], and the 1987 Frontal Eddy Dynamics Experiment (FRED) [*FRED Group*, 1989], with moorings respectively north and south of Cape Hatteras, were also tidally analyzed, and yield results consistent with those of the MMS data.

3. Hydrographic Setting

[10] Recent work on extended time series from the Hatteras shelf has highlighted the strong vertical and horizontal stratification near Cape Hatteras, owing to the wide variety of water types that impinge on the region [*Savidge and Bane*, 2001; *Flagg et al.*, 2002; *Gawarkiewicz et al.*, 1996; *Savidge*, 2002; *Ullman and Cornillon*, 1999]. In summertime, a strong contrast between subsurface cold-pool water and the near-surface warm layer exists throughout the MAB, extending southward as far as the study region. *Flagg et al.* [2002] have discussed the development of seasonal stratification north of Cape Hatteras, as the near-surface waters of the quite cold MAB shelf water are warmed in summer. SAB shelf water is less vertically stratified, though surface heating and limited freshwater runoff can lighten surface layers. The confluence of multiple water types at Cape Hatteras supports several strong mesoscale fronts (Figure 1) with strong horizontal and vertical density gradients in the region which affect the density field to first order. Specifically, both Middle Atlantic Bight (MAB) shelf water (cold and fresh) and South Atlantic Bight (SAB) water (warm and salty) converge on Cape Hatteras year-round, and support the strong Hatteras Front there, oriented cross shelf, and wrapping northeastward at the shelf edge [*Savidge and Bane*, 2001; *Churchill and Berger*, 1998; *Savidge*, 2002]. The cross-shelf portion migrates alongshelf under wind, Gulf Stream, and buoyancy forcing [*Savidge*, 2002; *Savidge and Austin*, 2007]. Seaward

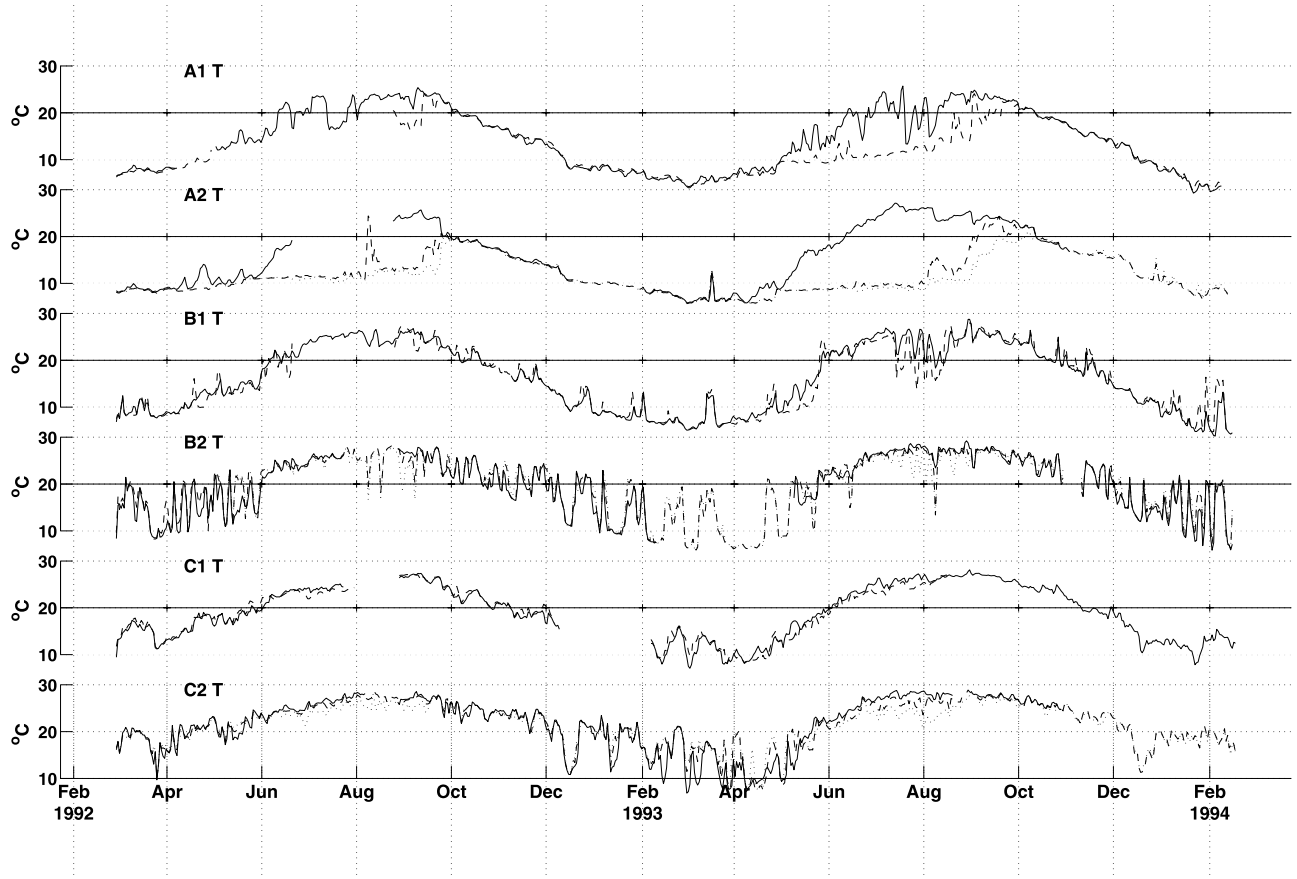

Figure 3. Temperature records (48HLP) from the shelf 20- and 35-m isobath moorings. For the 20-m isobath moorings (A1, B1, and C1; first, third, and fifth panels, respectively), near-surface (solid line) and near-bottom (dashed line) are shown. For the 35-m isobath moorings (A2, B2, and C2; second, fourth, and sixth panels, respectively), near-surface (solid line), middepth (dashed line), and near-bottom (dotted line) are shown.

of the shelf, the strong Gulf Stream front is evident, contrasting especially well with the MAB shelf water in both temperature and salinity. The contrast between Gulf Stream and SAB shelf water is less pronounced, but is enhanced in winter with the seasonal cooling of the shelf waters. The Gulf Stream is known to inject warm streamers into the shelf region at Cape Hatteras [*Churchill and Cornillon*, 1991; *Gawarkiewicz et al.*, 1990; G. Gawarkiewicz et al., manuscript in preparation, 2007], and influences the export of shelf water there [*Churchill and Berger*, 1998; *Ford et al.*, 1952; *Savidge and Bane*, 2001]. Additionally, two alongshelf oriented fronts in the region may affect stratification and support internal tides as well. The Shelf Break Front (SBF), aligned along the 200-m isobath, extends southward of 36°N latitude, where it converges upon the Gulf Stream and turns seaward [*Lozier and Gawarkiewicz*, 2001; G. Gawarkiewicz et al., manuscript in preparation, 2007]. Finally, the MAB Mid Shelf Front (MSF), has been identified farther north in the MAB along the 50-m isobath by *Ullman and Cornillon* [1999]. Examination of regional and seasonal front probability plots deduced from edge detection of satellite imagery suggests the MSF may extend southward of 36°N into the study region (D. S. Ullman, unpublished data, personal communication, 2002).

[11] The evolution of stratification along the shelf edge and on the shelf north and south of Cape Hatteras is now examined, using 48-HLP temperature time series from the moorings, and placed into context with what is known about the MSF, HF, GS, and SBF. Temperature data from the shelf edge north and south of Cape Hatteras reveals the contrast between the two regions through the year (Figure 2). In summer, the northern two shelf-edge stations, A3 and D1, exhibit quite strong vertical stratification. At 35 and 55-m depth on these 60-m isobath moorings, the sensors are imbedded in cold-pool water, while the shallowest meters at 5-m depth show warming in spring and summer due to air-sea heat fluxes, as described by *Flagg et al.* [2002]. In winter the warm surface layer disappears, and the water column is unstratified. Farther south at 60-m isobath shelf-edge mooring D2, the summertime top to bottom temperature difference is similar to that at A3 and D1, but the middepth temperature fluctuates between the two extremes, indicating this station is near the southernmost edge of outer shelf cold pool water, and that the structure of the vertical stratification here is more erratic. At the southern two shelf-

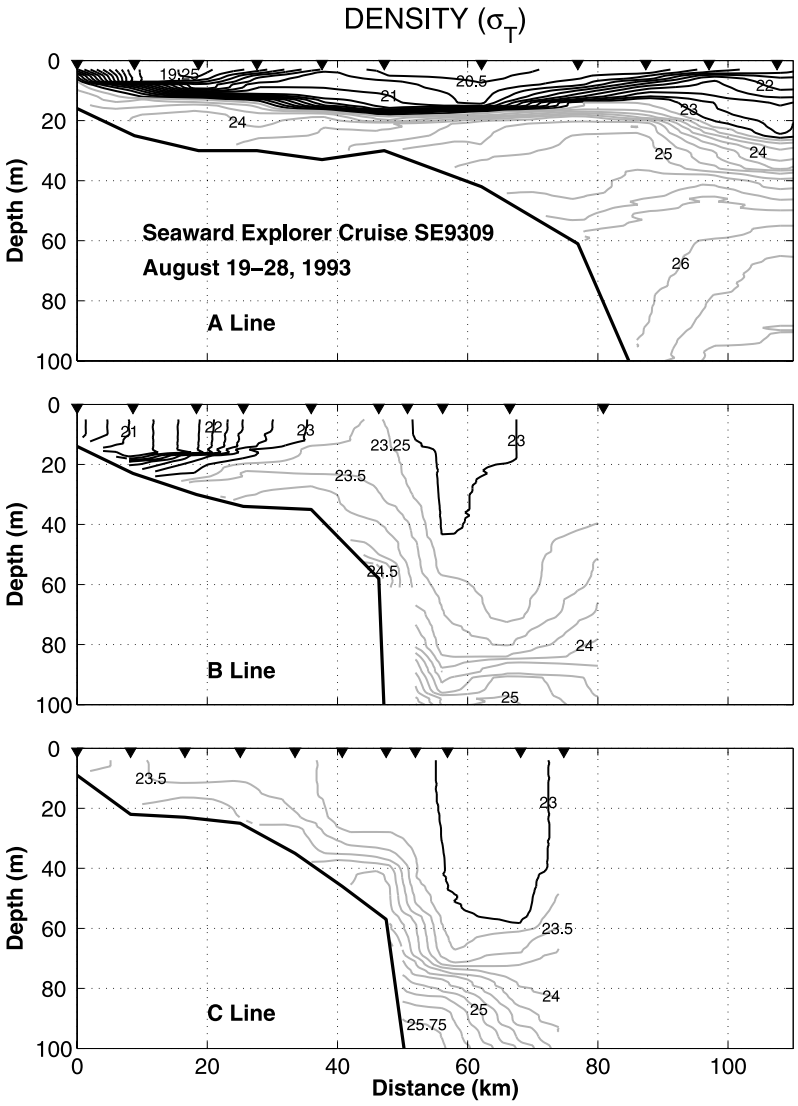

Figure 4. Density sections (σ_T) from August 1993 M/V *Seaward Explorer* cruise. Contour interval is 0.25 (σ_T); isopycnals of 23.25 and higher are plotted in gray.

edge stations, moorings B3 and C3, the stratification is of much smaller magnitude than at the northernmost two shelf-edge stations A3 and D1, since the deeper waters at B3 are not nearly so cold. Outer shelf cold-pool water seldom extends as far south as the B line in summer, but does extend to the B line closer to shore.

[12] Data from the 20- and 35-m isobath moorings (Figure 3) indicate strong summertime stratification across the shelf in the northern end of the study site (moorings A1 and A2) as seen for the northern shelf edge moorings A3 and D1. Stratification along the B and C lines is typically of much smaller magnitude. However, at B2 and especially at B1, a strong front crosses the mooring locations at frequent intervals in summer, with colder temperatures approaching those seen in the subsurface along the A line. Conversely, this front seldom appears in the summertime data from the C line, but does appear there in winter. This is consistent with the seasonal pattern of the Hatteras Front, which resides near or south of Cape Hatteras in winter, and typically farther north in summer under prevailing north-eastward summertime winds (two examples are shown in the work of *Savidge* [2002, Figure 9]). The front crosses the C2 and C1 moorings frequently during both winters, and also appears at the B2 mooring farther north in winter less frequently.

[13] Density sections from August 1993 ship transects along mooring lines A, B and C illustrate the large along-shelf gradient in stratification in summer (Figure 4). Along the northern A line (top panel), the very strong summer stratification indicated in the temperature time series plots is evident, with a sharp strong density gradient over the entire shelf, transitioning to a more diffuse stratification off the shelf in the seasonal thermocline. Notice that at the shelf break, the isopycnals slope steeply, opposing the direction of bathymetric slope. By the B line (middle panel), most of the cold pool water has exited the shelf, but the nose of the cool fresh MAB water extends past the B line nearshore, illustrated by the less dense nearshore waters ($\sigma_T \leq 23$), bounded underneath by a weak pycnocline. Along the C line, the shelf water is weakly stratified, typical of

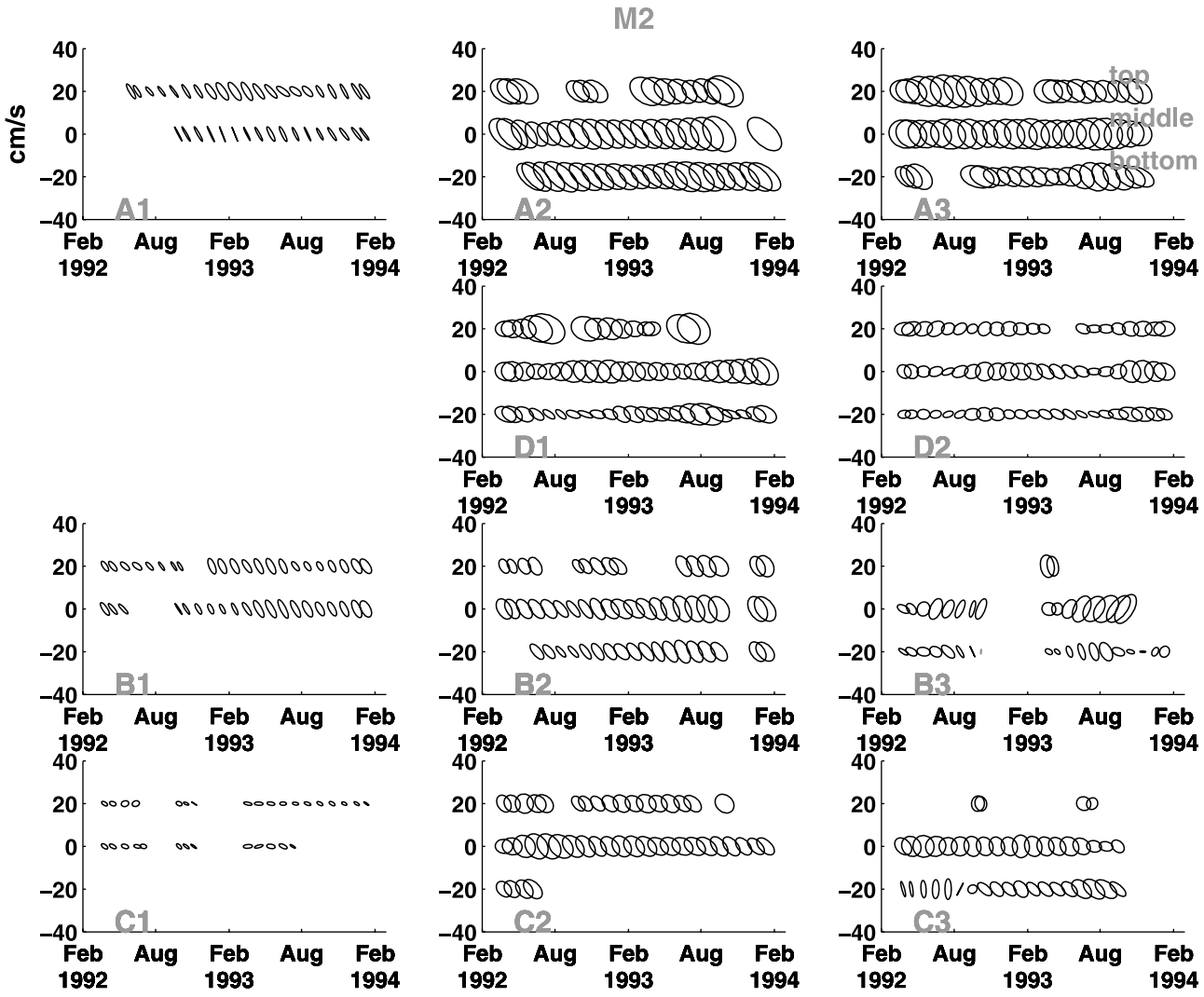

Figure 5. Running three-month M2 tidal ellipses at all shelf locations for all depths. Ellipses are offset by 20 cm/s to indicate the top, middle, and bottom current meters on the mooring, as labeled. Values that exceed twice the standard deviation are plotted in black; those that do not are plotted in gray.

summertime hydrography in the warm, salty waters of the SAB. Similar stratification is also evident over the outer shelf along the B line, between the nearshore MAB shelf water and the Gulf Stream. The cross-shelf density gradient changes sign over the outer shelf along the B line. The Gulf Stream is evident seaward of the shelf break along both the B and C lines, indicated by the lighter contours in the upper ocean and by the isopycnals below about 4-m depth, which trend downward to the east, approximately parallel to bathymetry.

[14] It should be emphasized that the hydrographic structure near Cape Hatteras, illustrated in Figure 4 here and in the work of *Savidge* [2002, Figures 9 and 10], can be considerably more complex than the examples shown, especially directly seaward of the Cape itself, where buoyancy, strong winds, and the Gulf Stream all affect circulation to first order. In this region many competing effects contribute to a complicated and variable horizontally and vertically stratified setting, which may have significant implications for the baroclinic tides and waves propagating over the shelf.

4. Semidiurnal

[15] The M2 semidiurnal is the largest tidal constituent over the record-long tidal analyses at all depths and locations on the shelf both north and south of Cape Hatteras, consistent with the *Lentz et al.* [2001] barotropic tidal analysis. Secondary constituents are N2, S2, K1, and O1, all at less than half the magnitude of the M2 tides for the overall records, but with large summertime magnitudes in K1 and O1 that approach those of the M2 tide, discussed below. A midshelf maximum is apparent in all five of these constituents, especially north of Cape Hatteras, as reported previously by *Lentz et al.* [2001].

[16] Tidal analyses of measured currents over running three-month subsections illustrate seasonal and spatial variability in the primary constituents. In the M2 constituent (Figure 5), an increase of about 5–10 cm/s of tidal ellipse

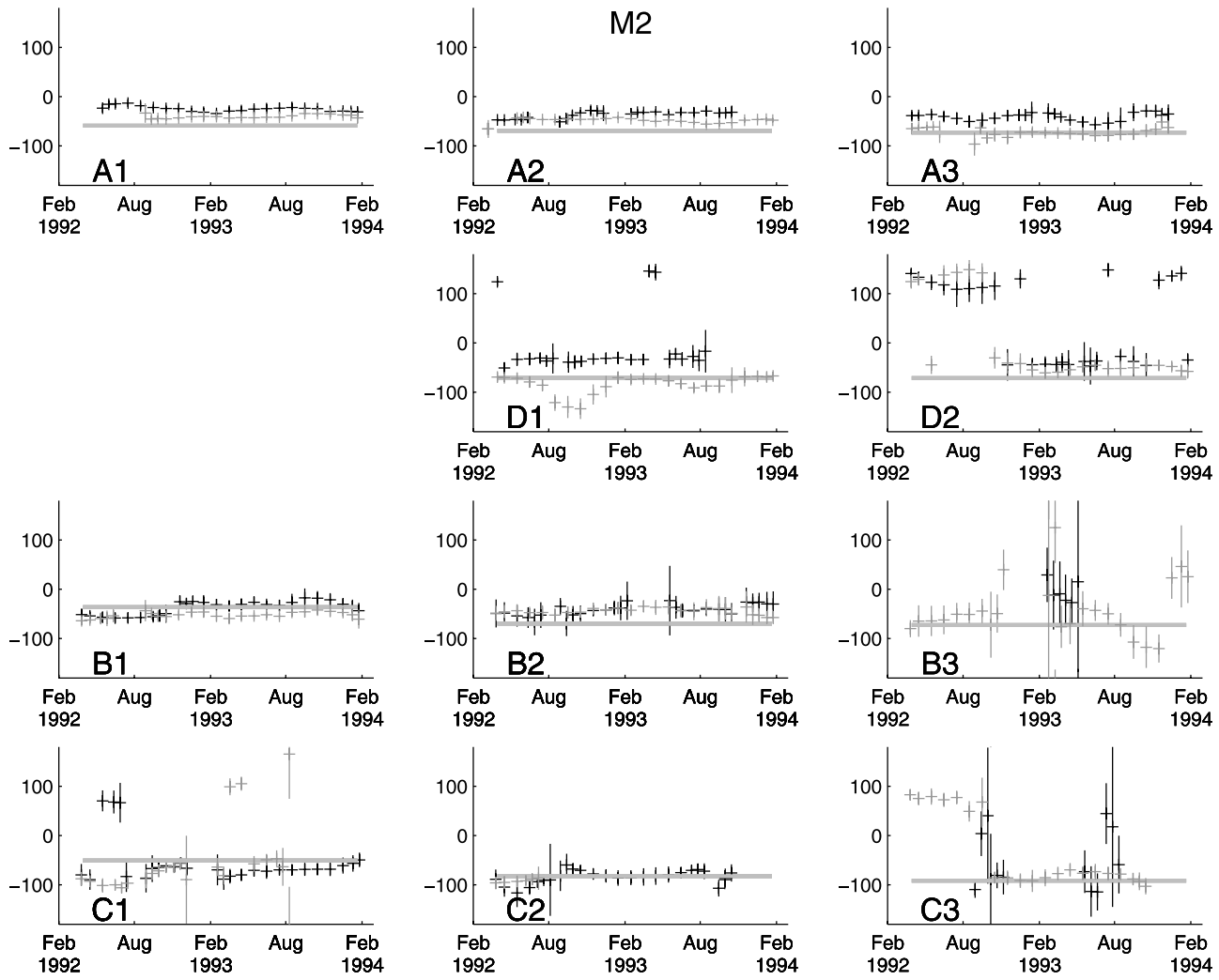

Figure 6. Running three-month M2 phase lags (degrees relative to GMT) at all shelf locations for all depths. Phases (crosses) and errors (vertical extensions of the crosses) are plotted such that error bars wrap around the panel at the bottom/top. Estimates from near-surface (black crosses) and near-bottom (gray crosses) at each mooring are shown, leaving out the middepth records for clarity. Gray horizontal bars in each panel show the Advanced Circulation (ADCIRC) model predicted phases.

magnitude is evident in summer at moorings D1, D2, and B3, all at the 60-m isobath. Slight variability (a few cm/s) with season also appears in the M2 at stations farther shoreward, at A1, A2, B1, B2, C1, and C2. Tidal ellipse orientation in the dominant M2 is fairly uniform with depth.

[17] Phase plots from observations show a bottom-to-surface phase lag of near 30°, or about an hour, in many locations (Figure 6; only near-surface and near-bottom data are shown for clarity), consistent with tidal boundary layer theory [*Soulsby*, 1990]. Apparent large jumps in phase (near 180°) at D2 and C3 are likely due to ambiguity in the ellipse estimation, and are not discussed. Alongshelf phase lags in observations are apparent along the 20- and 35-m isobaths, with the southern C1, C2 stations leading the northern A1, A2 stations by several tens of degrees. The observed phases are generally in good agreement with the ADCIRC-predicted phases, which are shown for comparison as horizontal bars in the figure panels.

[18] Using a fourth-order Butterworth filter, the 3HLP current data are filtered to pass the 9- to 15-hour frequency band, and the variance of this semidiurnal band is computed over the filtered time series. Figure 7 shows the vertical profiles of semidiurnal band variance along lines A and B, for June to September 1992 and 1993. The vertical profiles along line A (Figure 7, upper panels) show midshelf values that equal or exceed those at the shelf edge, with low values at the 20-m isobath. Along the B line in summer, despite large M2 amplitude at the shelf break, variance at the 35-m isobath is lower than along the A line (Figure 7, lower panels).

[19] For much of summer 1992, the vertical structure in the M2 variance profiles show a middepth minimum, consistent with the velocity profile shape of low-mode internal waves. In September 1992, the variance maximum near the bottom may indicate possible bottom-trapping. The situation is reversed in summer of 1993, with a bottom

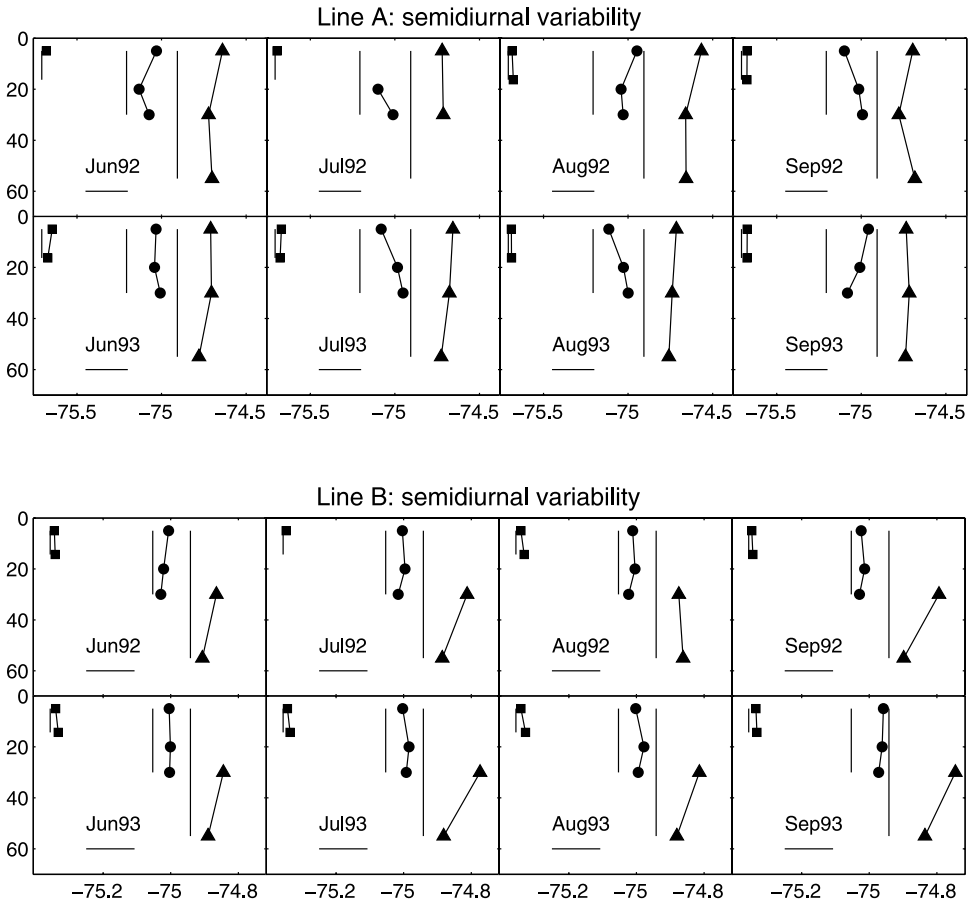

Figure 7. Semidiurnal (9- to 15-hour) variance profiles in the vertical across lines A (upper panels) and B (lower panels), computed by month. Variance in $cm^2\ s^{-2}$ is scaled to match the x-axis longitudinal range, so that plotted magnitudes are consistent between the mooring lines. A horizontal line indicating variance of 100 $cm^2\ s^{-2}$ is shown for reference.

maximum at A2 during June to August. Along line B, the midshelf profiles retain a frictional boundary layer structure over much of the year, and the shelf edge mooring holds the greatest variability in strength and shape over the deployment. The fact that these velocity data come from pointwise current meters in the vertical, not ADCPs, combined with the loss of near-surface current meter data at B3 over much of the measurement period prevents a more accurate estimate of vertical structure.

[20] Under summertime stratification, the seasonal signals in the tidal analysis and the vertical profiles along line A (Figure 7) suggest that the M2 internal tide can propagate shoreward at least to the 35 m isobath. Wavelength and phase speed of the propagating signal can be estimated with a dispersion relation for a simplified M2 internal tide. Assuming a hydrostatic, mode 1 wave under constant buoyancy frequency N and depth H, the dispersion relation is given by

$$\omega^2 = f^2 + \frac{kHN^2}{2\pi}\ , \qquad (1)$$

where ω is the frequency and k is the wavelength [*Gill*, 1982]. Evaluated at the A3 shelf break mooring ($H = 60$ m) using density from the August 1993 cruise, this yields wavelengths of 4.5–16.3 km and phase speeds of 10.0–36.3 cm/s for bottom and depth-averaged N^2, respectively.

[21] A likely generation site of the M2 internal tide observed on the shelf is the shoreward edge of the swath of supercritical slope that lines the continental margin. Using stratification observed over the August 1993 cruise (Figure 4), local estimates of the M2 critical slope suggest that it is subcritical through 6–12 and 3–5 km offshore of the 60-m isobath along the A line and B or C lines, respectively. *Lerczak et al.* [2003] caution that the horizontal scale of narrow continental shelves with steep margins compared to that of the internal tide may complicate the classification of internal tides along the shelf and shelf break. The supercritical slopes just offshore of the shelf break moorings appear to be controlled by the steepness of the slope rather than by stratification; such regions are proposed by *Lerczak et al.* [2003] to serve as the "natural boundary separating shelf and slope internal wave dynamics". Though beyond the scope of this paper examining shelf internal tides, tidal analysis of mooring data from the 2000- and 3000-m isobaths reveals patterns of M2 variability that differ from those of the shelf data. This finding may indicate reflection of incident internal tidal beams by supercritical

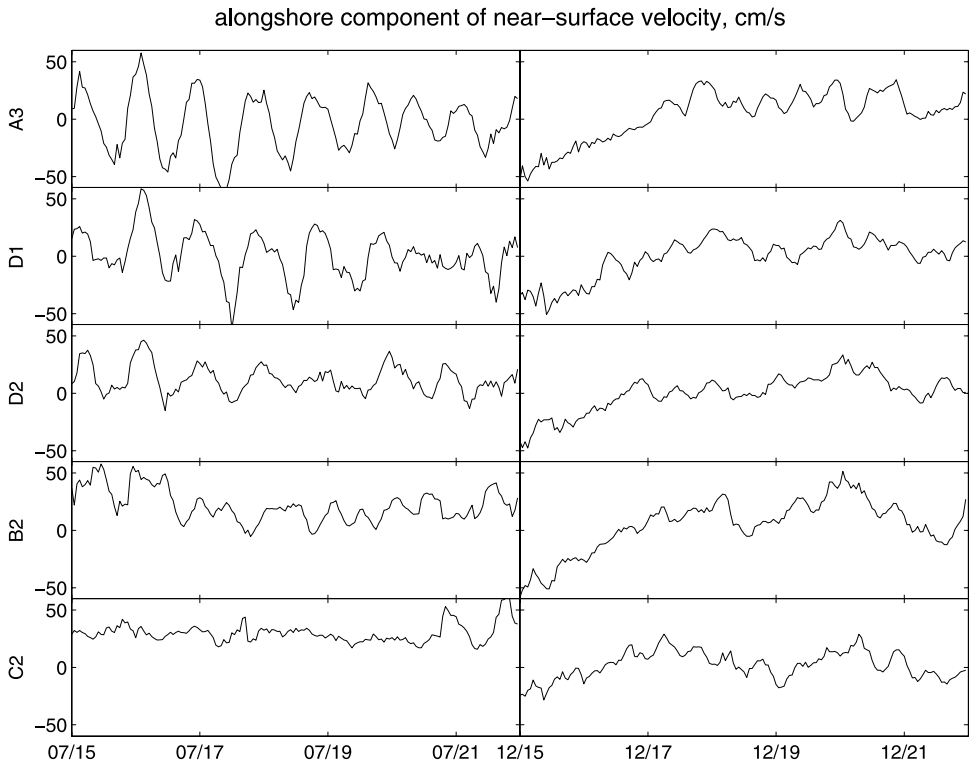

Figure 8. Time series of alongshore component of velocity.

slope as seen by *Nash et al.* [2004] off Virginia, at a location ~160 km north of Cape Hatteras.

[22] Along line B, M2 internal tide energy is much weaker at B2 than at B3, suggesting far less effective shoreward propagation along the B line. This may be due to weaker vertical stratification than along the A line, to effects from the presence of fronts on the shelf, or to weaker generation potential at the shelf edge owing to the isopycnal slope. Density sections and temperature time series (Figures 2–4) illustrate the strength and variability of stratification along the B line relative to the A line, both temporally and spatially. While the persistent strong summertime stratification along the A line (and farther north in the MAB) may provide a conduit for internal tidal energy to propagate onshore from the shelf edge, horizontal pathways of stratification do not appear as far south as the B line. The cross-shelf density gradient on the shelf associated with the Hatteras Front may even act as a barrier, dissipating, reflecting or refracting shelf edge M2 internal tidal energy at the frontal boundary, as discussed in the *Chen et al.* [2003] study of tidal propagation through fronts. Further, the generation of M2 internal tide energy at the shelf edge may differ between the A line and the B and C lines owing to the orientation of isopycnals at the shelf edge. Along the A line, isopycnals at the shelf edge slope upward in the seaward direction, in the opposite sense to bathymetry. Farther south, off lines B and C, the Gulf Stream resides adjacent to the shelf, and its associated isopycnals slope downward to the east, at an angle that is very nearly parallel with the bathymetric slope. As in the work of *Chuang and Wang* [1981] and *Chen et al.* [2003], such isopycnal orientation is less conducive to the generation of internal tides at the shelf edge than when isopycnal slope is in the opposite sense as bathymetric slope.

5. Diurnal

[23] Time series of the alongshore component of near-surface velocity over representative weeks in summer and winter (Figure 8) indicate the strength of the increase in the diurnal signal over an alongshore section of the array. During winter (right panels), the signal is dominated by the subtidal and the semidiurnal. In contrast, a typical week-long time series of near-surface velocity from the shelf-edge moorings during the summer indicates the diurnal variability is greatly enhanced north of Cape Hatteras at moorings A3, D1, and D2, reducing to the south.

[24] In the course of the running three-month tidal analysis of the data, large seasonal variability in the K1 and O1 diurnal tidal components was identified, with largest values in summer (K1 shown in Figure 9). O1 ellipses (not shown) are qualitatively similar but 10–25% smaller. The seasonal variability is most pronounced north of Cape Hatteras at shelf-edge moorings A3, D1, and D2, with only minor variation in time at locations south of Cape Hatteras. Observations match ADCIRC K1 magnitudes in winter, but are much larger in summer. It is unlikely that the observed seasonal variability in the diurnal constitutes a diurnal internal tide: at these latitudes, the diurnal internal tide is subinertial and cannot propagate through the region without significant anticyclonic shear (1–2 m/s over 50 km) to open up the frequency band available to propagate an internal tide at O1 or K1. Shear in frontal jets in the region can be large, but is patchy in space (the fronts and associated jets are typically 10 km wide), and likely does

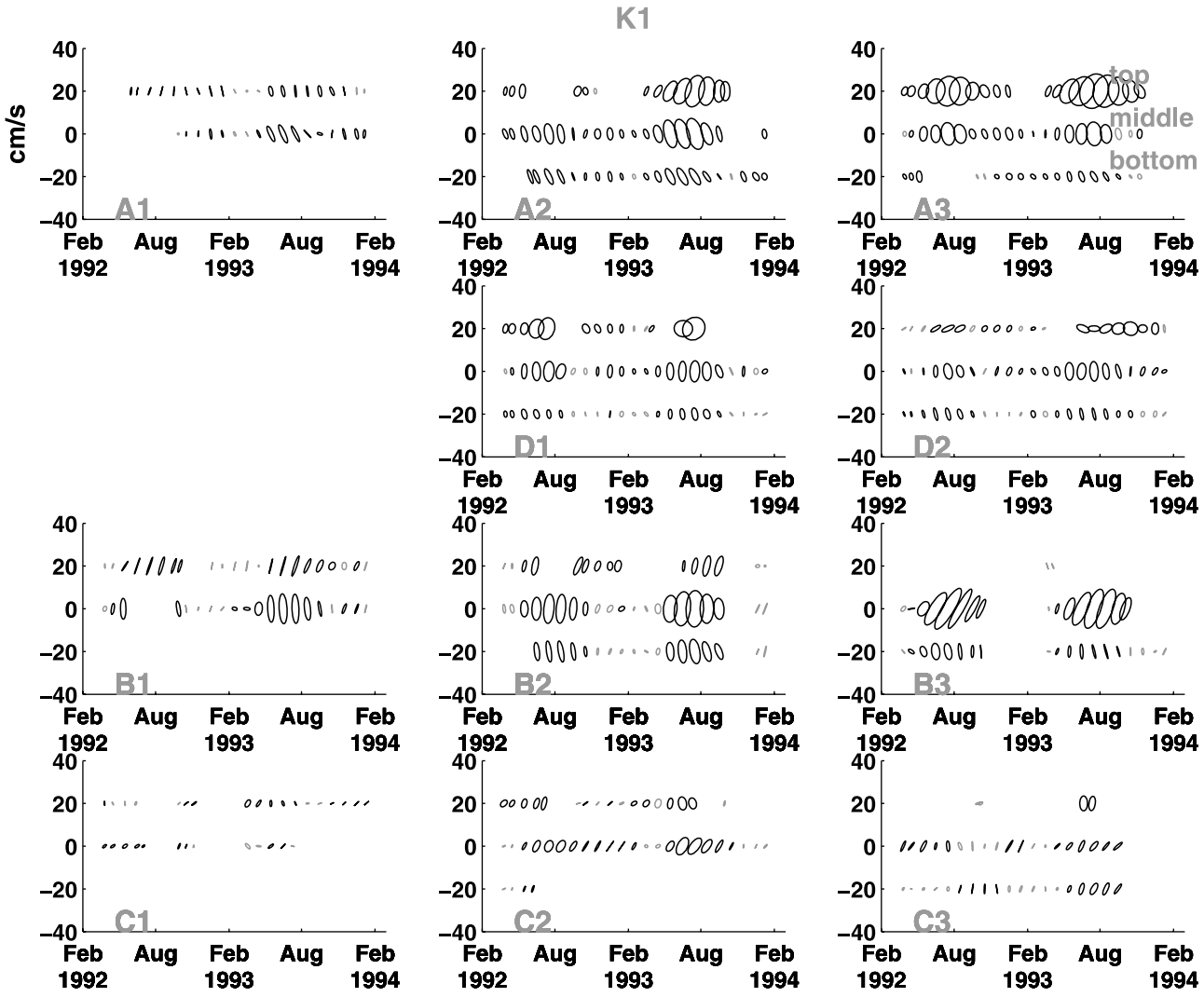

Figure 9. Running three-month K1 tidal ellipses at all shelf locations for all depths. Panel placement roughly corresponds to geographic location, though please note that both moorings D1 and D2 were along the 60-m isobath between moorings A3 and B3, so their panel placement is slightly misleading. Ellipses are offset by 20 cm/s to indicate the top, middle, and bottom current meters on the mooring, as labeled. Values that exceed twice the standard deviation are plotted in black; those that do not are plotted in gray.

not change the effective f on large enough spatial scales to support internal tide propagation. It is possible that the O1 and K1 barotropic currents could force a baroclinic tide trapped at the shelf break. However, if the magnitude of the K1 and O1 currents under well-mixed conditions represents potential barotropic forcing, it is much smaller than the observed potential response under stratification. In the following, spectral analysis is employed to further investigate if the seasonal appearance of this diurnal band variability is consistent with a subinertial mechanism such as coastally trapped waves.

[25] Using a sixth-order Butterworth filter to exclude the local inertial (20.2- to 21.0-hour periods over the mooring array), diurnal-band variance is constructed as above for the semidiurnal, taken over the 22- to 26-hour band-passed currents. The magnitude of vector variance of near-surface velocity is shown by month over the 25-month deployment (Figure 10). Summer months show maximum diurnal variance at the shelf break locations, with markedly less activity inshore and along the C line.

[26] Variability in the 22- to 26-hour band is highly correlated in the alongshelf direction, along both the 60- and 35-m isobaths. Cross spectra of the alongshore component of velocity at shelf-edge moorings A3, D1, D2, and B2 are computed using 256-hour Hanning window with a 50% overlap. (Near-surface data at B3 are not available over much of the study period owing to instrument failures.) The upper panels of Figure 11 show cross-spectral power density estimates of alongshore velocity across the alongshore section for summer and winter (June to August 1992 and December 1992 to February 1993), which generally resemble the autospectra of each time series under the same windowing (not shown). Winter cross-spectral power contains significant peaks in the synoptic band and at the

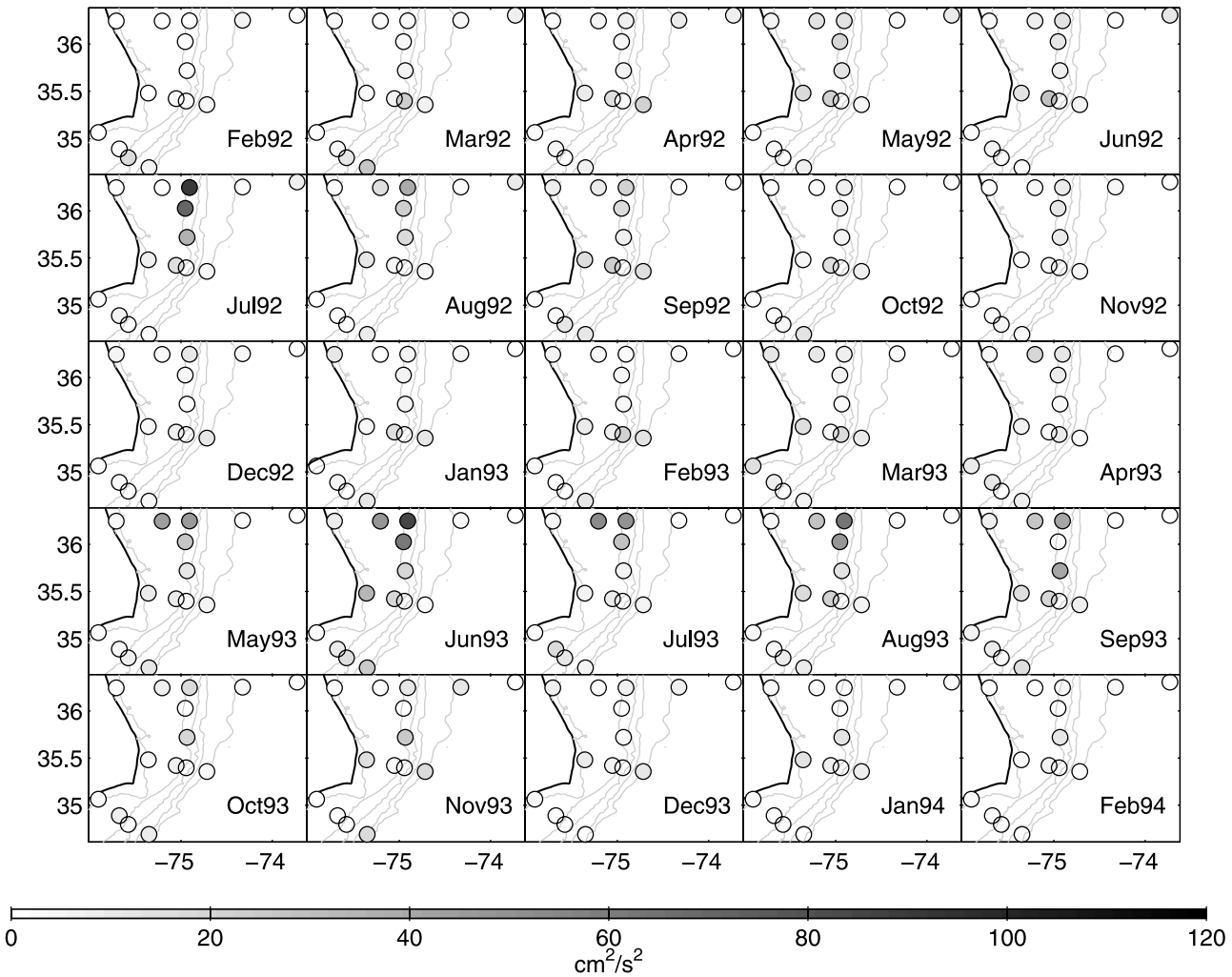

Figure 10. Diurnal-band variance of near-surface velocity ($cm^2\ s^{-2}$), shown by month. The 20-, 50-, 200-, 1000-, and 2000-m isobaths are shown in gray for reference.

semidiurnal, but summer cross-spectral power is characterized by two large spectral peaks in power at the diurnal and inertial frequencies. The power in the synoptic band decreases by nearly an order of magnitude, and power in the diurnal/inertial band increases by the same, almost giving the appearance of a spectral gap between the diurnal and lower frequencies. The summertime diurnal and inertial peaks appear to be distinct from each other, but fall off slowly toward lower and higher frequencies, respectively.

[27] Estimates of coherence that exceed the 95% confidence level (plotted in Figure 11c) allow for meaningful estimates of phase differences of the cross-spectral estimates, which are shown in the lower right panel of Figure 11. Phase is relatively constant over the diurnal band, with a pronounced offset among the mooring pairs. The analysis is repeated by season over the length of the deployment, converting significant phase estimates to lags and averaging over the diurnal band (22–26 hours). Estimates of alongshore phase speed are made by season with a linear regression of phase lags and distance between the moorings, shown in Figure 12. Lags are color-coded by the cross-spectral power of the indicated moorings, taken as an average over the diurnal band as above. Independent estimates of phase lag using cross correlation of raw alongshelf currents (not shown) verify the phase lags derived from cross-spectral analysis. The regression statistics indicate only two seasons with significant estimates of phase speed over the shelf break section: summer 1992 and summer 1993, both of which contain the greatest cross-spectral power in the diurnal band, with estimated southward phase speeds of 2.4–2.6 m/s. However, the 95% confidence intervals about these values approach 75% of the estimate; the temporal resolution (generally 1 hour) of the mooring data constrains the ability to improve uncertainty, particularly over short distances where the cross-spectral power is highest. Parallel analysis based on near-surface and middepth 60- and 35-m isobath mooring velocities yield similar estimates, with greater values and uncertainties inshore of the shelf break moorings.

[28] Coastally trapped waves are presented as a mechanism to explain the increased variability in the diurnal band under summertime stratification. Under well-mixed conditions, the diurnal band (O1 $\approx 0.8f$, K1 ≈ 0.84–$.88f$) is too close to the inertial for coastally trapped wave propagation.

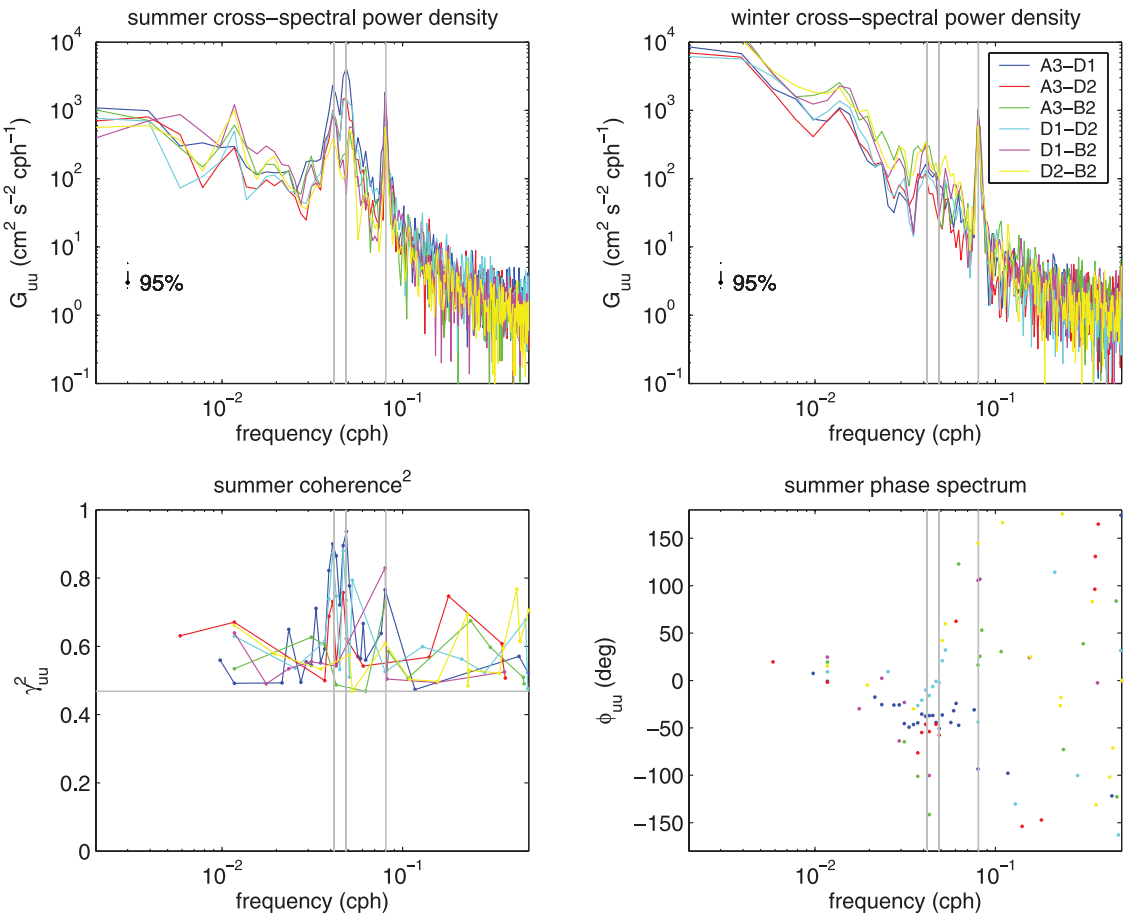

Figure 11. Cross-spectral power of alongshore component of near-surface velocity for (a) summer and (b) winter. Line color gives the pairing of moorings along the shelf break, and the error bar denotes the largest 95% confidence interval over the cross spectra plotted. (c) Coherence above the 95% confidence level (marked in gray) is shown for the summer time series, as well as (d) the phases which correspond to coherence significant to 5%. Gray vertical lines indicate the K1, inertial (local for 36°N), and M2 frequencies.

Stratification increases the resultant frequency at a given wave number, as described in the work of *Brink* [1991, Figure 2]. *Huthnance* [1978] defines A, a measure of stratification and bathymetric slope that shows whether the coastally trapped wave frequency will reach the local inertial frequency. If the cross-shore maximum of A ($\equiv |\frac{N}{f}\frac{\partial h}{\partial x}|$), evaluated at the bottom, is greater than or equal to unity, then coastally trapped waves of frequency f are admitted. Figure 13 shows estimates of $N^2(z)$ evaluated at the bottom, at its maximum, and the depth average, derived from the density sections in Figure 4. Assuming this section is representative of summertime stratification, the cross-shore profile of A indicates that the near-bottom stratification is sufficient to support a coastally trapped wave of frequency f along lines A and B. By extension, the stratification at the shelf edge moorings appears to be great enough to support diurnal coastally trapped waves at $0.84-.88f$.

[29] The form of the coastally trapped waves under stratification can be represented with the Burger number S ($\equiv \frac{N^2H^2}{f^2L^2}$). *Huthnance* [1978] defines two regimes of coastally trapped waves under stratification: small S, where the waves approach the form of barotropic continental shelf waves, and large S, under which the waveform approaches that of internal Kelvin waves. The value of S is calculated at the shelf break and slope along lines A, B, and C for shelf width L, deep sea depth H, and the estimates of stratification derived from the density sections in Figure 4. Considering near-bottom and depth-averaged N^2, S is on the order of 2–10 and 10–100 along lines A and B. At the 60-m isobath, S is estimated to be approximately 80, 115, and 60 at A3, D1/D2, and B3 (the estimate of S at D1/D2 is constructed from an August 1993 cross-shelf transect that bisected the D line at the shelf break.) In this large S regime, coastally trapped waves are greatly modified by stratification, and the nondimensional dispersion relation for each mode $m > 0$ becomes linear:

$$\sigma(k) = \frac{kS^{1/2}\int_{-1}^{0} n\,dz}{m\pi}, \tag{2}$$

where σ, k, n, and z are the nondimensional frequency, horizontal wave number, buoyancy frequency, and vertical coordinate, respectively. Figure 13c shows the dispersion of

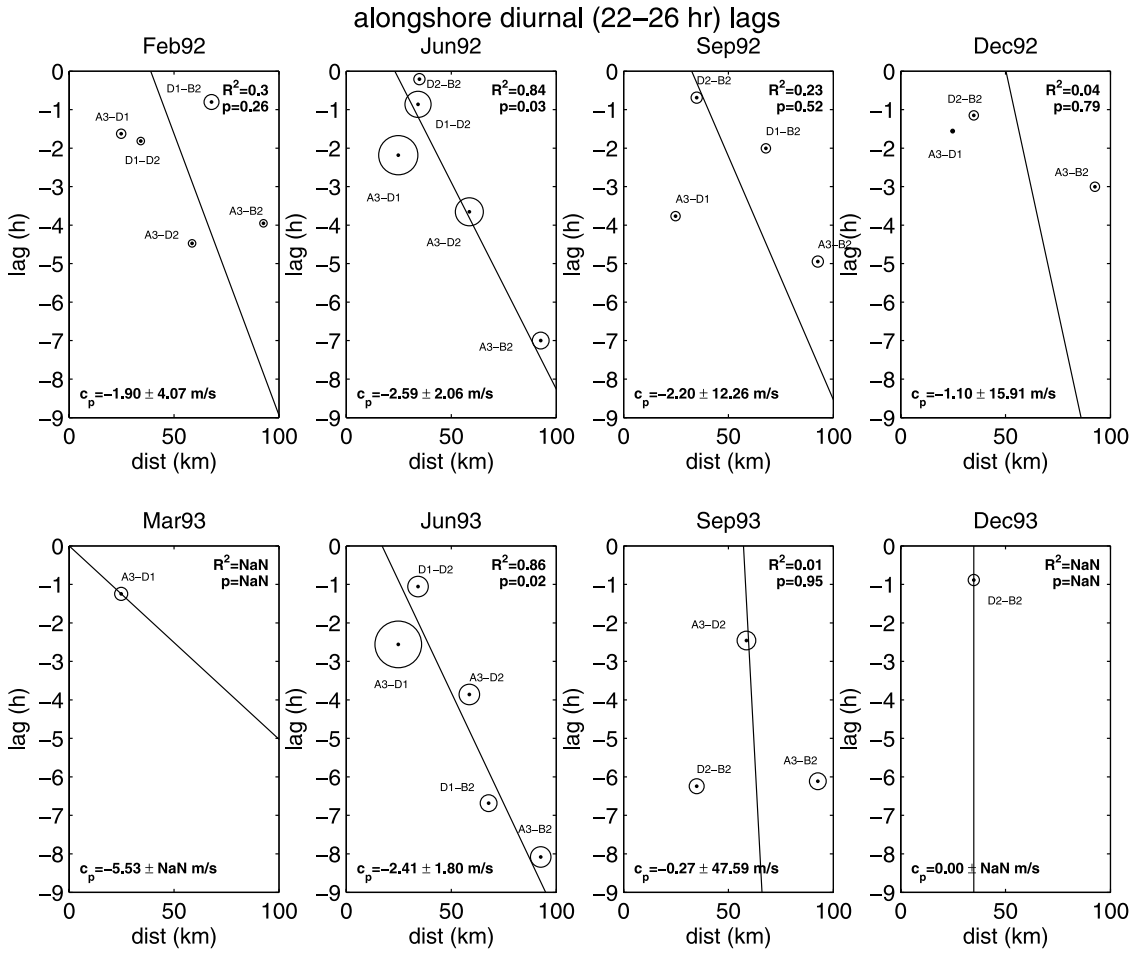

Figure 12. Alongshelf lags of the local alongshore component of velocity, as derived from cross-spectral phase estimates in the diurnal band (22–26 hours) in Figure 11, given by season. The best fit line from a linear regression, its statistics, 95% confidence intervals, and derived phase speed are shown.

modes 1 and 2 under near-bottom and depth-averaged N^2 along the 60-m isobath. As expected, the effect of stratification/mode number is to increase/decrease frequency and phase speed. Theoretical phase speeds along line A are shown in Figure 13d for locations near and seaward of the shelf break. The observed wave number, frequency, and phase speed are consistent with the wave characteristics of the mode 1 baroclinic coastally trapped wave under the bulk average measure of water column stratification over the shelf break and slope.

[30] The analysis above is consistent with baroclinic CTWs, and points to the first observations of diurnal coastally trapped waves in the Cape Hatteras study region. Diurnal CTW's have been observed in other locations, for example off Scotland [*Cartwright*, 1969], off Vancouver Island [*Crawford and Thomson*, 1984; *Cummins et al.*, 2000; *Foreman and Thomson*, 1997], on the East Australian shelf [*Freeland*, 1982], and more recently on the Greenland shelf [*Lam*, 1999] and off the Kuril Islands [*Rabinovich and Thomson*, 2001]. *Freeland* [1982] may serve as a valuable basis for comparison to the present study, with dispersion curves calculated for lines of moorings between 33 and 38°S latitude. Topography and latitude along line A are qualitatively similar to those of Freeland's line 1, and yield comparable estimates of wavelength and phase speed. Wavelengths and alongshelf phase speeds are a bit smaller off Cape Hatteras than found on the southeastern Australian Shelf (200–250 versus 268-km wavelength and 2.4–2.6 versus 3.17–3.87 m/s, respectively), but the uncertainty in the present phase speeds estimates is noted.

[31] As in the work of *Crawford and Thomson* [1982], the diurnal barotropic tide is proposed as the mechanism forcing the propagation alongshelf. The generation site need not be local, but could be somewhere well north of the A line. *Daifuku and Beardsley* [1983] suggest the presence of a southward propagating mode 1 shelf wave in the MAB between latitudes 39–46°N, based on a model which fit shelf pressure data to a barotropic Kelvin wave and a mode 1 shelf wave. However, *Daifuku and Beardsley* [1983] consider only barotropic modes and ignore effects of stratification, which can be significant along much of the MAB shelf. The results shown here indicate that while *Daifuku and Beardsley* [1983] may account for a diurnal barotropic shelf wave mode in the MAB, diurnal barotropic CTWs appear to be excluded in the Cape Hatteras region owing to changes in shelf width. Though the barotropic tidal forcing remains available as potential forcing yearlong in the MAB, the development of seasonal stratification in

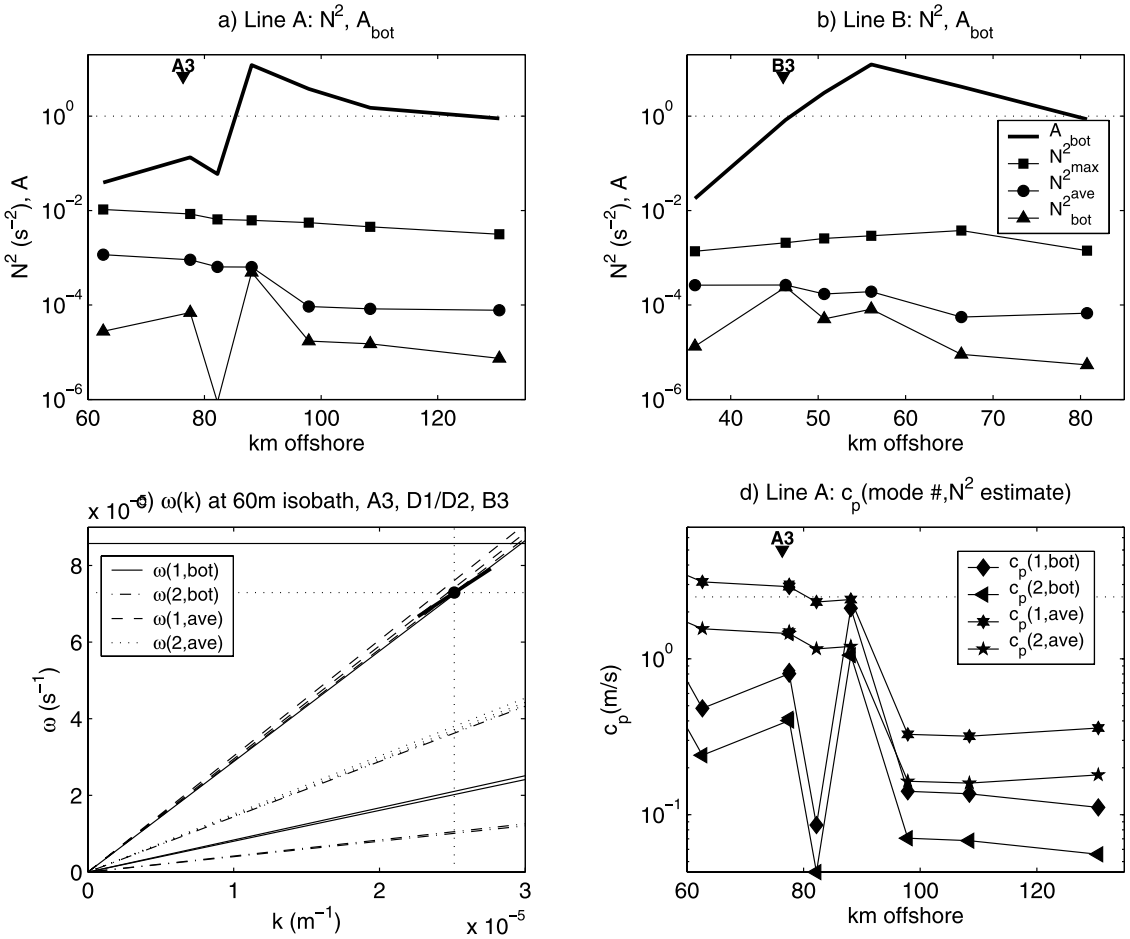

Figure 13. (a and b) Cross-shore profiles of N^2 evaluated at the maximum (squares), depth average (circles), and near-bottom (triangles) on the shelf break and slope along lines A and B. The thick line is the cross-shore profile of A, evaluated at the bottom. The inverted triangles show the location of the 60-m isobath moorings. (c and d) Dispersion relations and phase speeds are shown for large-S internal Kelvin-like coastally trapped waves along the 60-m isobath at A3, D1/D2, and B3. The lines are calculated for modes 1 and 2 given bottom and depth-averaged estimates of N^2. The local inertial and K1 frequencies are marked, and the vertical dotted line indicates the observed wave number k_{obs}.

summer may boost the dispersion relation sufficiently to allow the admittance of K1 at Cape Hatteras as a baroclinic mode resembling an internal Kelvin wave.

[32] While this analysis supports the southward propagation of diurnal coastally trapped waves at the shelf break north of Cape Hatteras, the mechanism for their extinction between the B and C lines is not certain. The *A* parameter evaluated along line C indicates that the stratification at the shelf break of line C is sufficient to support diurnal CTWs, but the Burger number *S* on the shelf is generally between 10 and 20% of the value calculated along lines A and B. It is unclear whether the waves evanesce from some location north of the study array or are arrested at Cape Hatteras due to potential effects of coastline orientation or friction.

[33] Subtidal CTWs have been examined previously in both the MAB [*Wang*, 1979] and the SAB [*Mysak and Hamon*, 1969; *Schwing et al.*, 1988; *Pietrafesa and Janowitz*, 1980, and references therein]. While the existence of CTWs in the MAB has not been disputed [*Wang*, 1979; *Brooks*, 1979], their presence in the SAB is sporadic and patchy at best. Whether subtidal CTWs from the MAB propagate southward past Cape Hatteras into the SAB has been debated in the literature. *Brooks* [1979] found significant coherence between the SAB and MAB at several-day and 1- to 2-week periods extending 200–400 km north or south of Cape Hatteras, but alongshelf phase lags in the SAB were near zero, which *Brooks* [1979] characterizes as "murky, at best" support for alongshelf CTW propagation. *Brink* [1990] examined CTW in the presence of friction and a mean current against the direction of CTW phase propagation, and surmised that even in the absence of a northward mean current in the SAB, the friction on the shelf alone would disallow southward propagation of CTWs past Cape Hatteras. There are also suggestions that large changes in coastline or bathymetric orientation alongshelf, as found at Cape Hatteras, would inhibit CTW propagation [*Brink*, 1991]. This data set further suggests the failure of diurnal period baroclinic CTWs to propagate from the MAB past the sharp bend at Cape Hatteras into the reduced stratifica-

tion, mean northward current and shallow frictional shelf of the SAB.

6. Summary

[34] Seasonal variability has been identified on the shelf near Cape Hatteras in the semidiurnal and diurnal frequency bands, from running three-month tidal fits to data from a two-year mooring array. The seasonally large semidiurnal variability appears to be an internal M2 tide whose propagation shoreward north of Cape Hatteras is supported by strong MAB seasonal stratification. At the southern end of the MAB and southward into the SAB, where seasonal summertime stratification is much weaker, the M2 internal tide does not propagate shoreward as effectively. The summertime magnitudes of the diurnal tidal components can become as large as the M2 north of Cape Hatteras, but are smaller south of the Cape. Cross-spectral analysis indicates alongshore southward propagation of the diurnal signal alongshelf as far south as Cape Hatteras, with a phase speed of 2.4–2.6 m/s along the 60-m isobath, though the uncertainty of the calculated phase speed approaches 75% of the calculated estimate. Very little energy in the diurnal frequency band propagates past Cape Hatteras.

[35] It is unlikely that the seasonal appearance of this variability in the diurnal constitutes a diurnal internal tide, since at these latitudes (34.5–36.5N), the diurnal frequency is subinertial. Coastally trapped waves (CTWs) are examined as a potential mechanism to explain the signals. While the diurnal band is too close to the inertial for CTW propagation under well-mixed conditions, stratification may increase the resultant frequency at a given wave number, as described in the work of *Brink* [1991]. The nature and cross-shelf and alongshelf extent of the strong stratification north of Cape Hatteras in summer is examined, and is consistent with the spatial variability seen in both the semidiurnal and diurnal signals. Estimates of the *Huthnance* [1978] stratification and slope parameter A yield large values, indicating that CTWs of diurnal frequency are possible in the study site both north and south of Cape Hatteras, but the values are much larger north of the Cape. The Burger number S has also been estimated for representative density fields on the shelf break, and these estimates suggest the summertime diurnal signal is consistent with baroclinic CTWs. If so, these are the first observations of diurnal CTWs in the Cape Hatteras study region.

[36] It has recently become clear that many features of the subtidal circulation at Cape Hatteras depend on variability in the density field, with both temperature and salinity playing important roles in controlling vertical and horizontal density gradients [*Lentz*, 2001; *Churchill and Berger*, 1998; *Savidge*, 2002; *Savidge and Austin*, 2007; *Churchill and Cornillon*, 1991; G. Gawarkiewicz et al., manuscript in preparation, 2007]. The variation of the semidiurnal and diurnal variability with season shown here is further evidence that the density field is of great importance in this region. Ultimately, modeling the Hatteras Shelf will require not only the use of realistic bathymetry and density gradients in both the vertical and horizontal, but also the temporal variability of the frontal positions, in order to approach accurate representations of circulation at Cape Hatteras.

[37] **Acknowledgments.** Support for D. K. Savidge and M. Santana came from the Center for Coastal Physical Oceanography and from the National Science Foundation (NSF) MUST REU program, both at Old Dominion University, and from NSF grant OCE-0406543. C. R. Edwards is supported by the Royster Society of Fellows and by ONR funding for the Southeast Atlantic Coastal Observing System (SEACOOS). The Minerals Management Service (MMS) data were collected under OCS study MMS 94-0047. Frontal Eddy Dynamics Experiment (FRED) and Ocean Margins Project (OMP) data were supplied courtesy of Peter Hamilton and Charles N. Flagg, respectively. Brian Blanton supplied code to interpolate Advanced Circulation (ADCIRC) tidal predictions to exact locations and times on the shelf.

References

Baines, P. G. (1982), On internal tide generation models, *Deep Sea Res., Part A*, *29*, 307–338.

Berger, T. J., P. Hamilton, R. J. Wayland, J. O. Blanton, W. C. Boicourt, J. H. Churchill, and D. R. Watts (1995), A physical oceanographic field program offshore North Carolina, *Tech. Rep. OCS Study MMS 94-0047*, Miner. Manage. Serv., U. S. Dep. of the Inter., New Orleans, La.

Blanton, B. O., F. E. Werner, H. E. Seim, R. A. Luettich Jr., D. R. Lynch, K. W. Smith, G. Voulgaris, F. M. Bingham, and F. Way (2004), Barotropic tides in the South Atlantic Bight, *J. Geophys. Res.*, *109*, C12024, doi:10.1029/2004JC002455.

Brink, K. H. (1990), On the damping of free coastal-trapped waves, *J. Phys. Oceanogr.*, *20*, 1219–1225.

Brink, K. H. (1991), Coastal-trapped waves and wind-driven currents over the continental shelf, *Annu. Rev. Fluid Mech.*, *23*, 389–412.

Brooks, D. A. (1979), Coupling of the Middle and South Atlantic Bights by forced sea level oscillations, *J. Phys. Oceanogr.*, *9*, 1304–1311.

Cartwright, D. E. (1969), Extraordinary tidal currents near St. Kilda, *Nature*, *223*, 928–932.

Chen, D., H. W. Ou, and C. Dong (2003), A model study of internal tides in coastal frontal zone, *J. Phys. Oceanogr.*, *33*, 170–187.

Chuang, W.-S., and D.-P. Wang (1981), Effects of density front on the generation and propagation of internal tides, *J. Phys. Oceanogr.*, *11*, 1357–1374.

Churchill, J. H., and T. J. Berger (1998), Transport of Middle Atlantic Bight shelf water to the Gulf Stream near Cape Hatteras, *J. Geophys. Res.*, *103*, 30,605–30,622.

Churchill, J. H., and P. C. Cornillon (1991), Gulf Stream water on the shelf and upper slope north of Cape Hatteras, *Cont. Shelf Res.*, *11*, 409–431.

Crawford, W. R., and R. E. Thomson (1982), The generation of diurnal-period shelf waves by tidal currents, *J. Phys. Oceanogr.*, *12*, 635–643.

Crawford, W. R., and R. E. Thomson (1984), Diurnal-period continental shelf waves along Vancouver Island: A comparison of observations with theoretical models, *J. Phys. Oceanogr.*, *14*, 1629–1646.

Cummins, P. F., D. Masson, and M. G. G. Foreman (2000), Stratification and mean flow effects on diurnal tidal currents off Vancouver Island, *J. Phys. Oceanogr.*, *30*, 15–30.

Daifuku, P. R., and R. C. Beardsley (1983), The K1 tide on the continental shelf from Nova Scotia to Cape Hatteras, *J. Phys. Oceanogr.*, *13*, 3–17.

Edwards, C. R., and H. E. Seim (2007), EOF analysis as a method to separate barotropic and baroclinic velocity structure in shallow water, *J. Atmos. Oceanic Technol.*, in press.

Flagg, C. N., L. J. Pietrafesa, and G. L. Weatherly (2002), Springtime hydrography of the southern Middle Atlantic Bight and the onset of seasonal stratification, *Deep Sea Res., Part II*, *49*, 4297–4329.

Ford, W. L., J. R. Longard, and R. E. Banks (1952), On the nature, occurrence and origin of cold low salinity water along the edge of the Gulf Stream, *J. Mar. Res.*, *11*, 281–293.

Foreman, M. (1977), Manual for tidal heights analysis and prediction, *Tech. Rep. Pac. Mar. Sci. Rep. 77-10*, Inst. of Ocean Sci., Patricia Bay, Sidney, B. C., Canada.

Foreman, M. (1978), Manual for tidal currents analysis and prediction, *Tech. Rep. Pac. Mar. Sci. Rep. 77-10*, Inst. of Ocean Sci., Patricia Bay, Sidney, B. C., Canada.

Foreman, M., and R. Thomson (1997), Three-dimensional model simulations of tides and buoyancy currents along the west coast of Vancouver Island, *J. Phys. Oceanogr.*, *27*, 1300–1325.

FRED Group (1989), Frontal Eddy Dynamics (FRED) experiment off North Carolina, *Tech. Rep. OCS Stud. MMS 86-0082*, Miner. Manage. Serv., U. S. Dep. of the Inter., New Orleans, La.

Freeland, H. J. (1982), Diurnal coastal-trapped waves on the East Australian continental shelf, *J. Phys. Oceanogr.*, *12*, 690–694.

Gawarkiewicz, G., R. K. McCarthy, K. Barton, A. K. Masse, and T. M. Church (1990), A Gulf Stream–derived pycnocline intrusion on the Middle Atlantic Bight shelf, *J. Geophys. Res.*, *95*, 22,305–22,313.

Gawarkiewicz, G., T. G. Ferdelman, T. M. Church, and G. W. Luther (1996), Shelfbreak frontal structure on the continental shelf north of Cape Hatteras, *Cont. Shelf Res.*, *16*, 1751–1773.

Gill, A. E. (1982), *Atmosphere-Ocean Dynamics*, 662 pp., Elsevier, New York.

Godin, G. (1972), *The Analysis of Tides*, 264 pp., Univ. of Toronto Press, Toronto, Ont., Canada.

Holloway, P. E., P. G. Chatwin, and P. Craig (2001), Internal tide observations from the Australian north west shelf in summer 1995, *J. Phys. Oceanogr.*, *31*, 1182–1199.

Huthnance, J. M. (1978), On coastal-trapped waves: Analysis and numerical calculation by inverse iteration, *J. Phys. Oceanogr.*, *8*, 74–92.

Lam, F.-P. A. (1999), Shelf waves with diurnal tidal frequency at the Greenland shelf edge, *Deep Sea Res., Part I*, *46*, 895–923.

Legg, S. (2004), Internal tides generated on a corrugated continental slope. Part I: Cross-slope barotropic forcing, *J. Phys. Oceanogr.*, *34*, 156–173.

Lentz, S. J. (2001), The influence of stratification on the wind-driven cross-shelf circulation over the North Carolina shelf, *J. Phys. Oceanogr.*, *31*, 2749–2760.

Lentz, S. J., M. Carr, and T. H. C. Herbers (2001), Barotropic tides on the North Carolina shelf, *J. Phys. Oceanogr.*, *31*, 1843–1859.

Lerczak, J. A., C. D. Winant, and M. C. Hendershott (2003), Observations of the semidiurnal internal tide on the southern California slope and shelf, *J. Geophys. Res.*, *108*(C3), 3068, doi:10.1029/2001JC001128.

Lozier, M. S., and G. Gawarkiewicz (2001), Cross-frontal exchange in the Middle Atlantic Bight as evidenced by surface drifters, *J. Phys. Oceanogr.*, *31*, 2498–2510.

Luettich, R. A., Jr., J. J. Westerink, and N. W. Scheffner (1992), ADCIRC: An advanced three-dimensional circulation model for shelves coasts and estuaries, report 1: Theory and methodology of ADCIRC-2DDI and ADCIRC-3DL, *Dredging Res. Program Tech. Rep. DRP-92-6*, 137 pp., U. S. Army Eng. Waterw. Exp. Stn., Vicksburg, Miss.

Mysak, L. A., and B. V. Hamon (1969), Low-frequency sea level behavior and continental shelf waves off North Carolina, *J. Geophys. Res.*, *74*, 1397–1405.

Nash, J. D., E. Kunze, J. M. Toole, and R. W. Schmitt (2004), Internal tide reflection and mixing on the continental slope, *J. Phys. Oceanogr.*, *34*, 1117–1134.

Pawlowicz, R., B. Beardsley, and S. Lentz (2002), Classical tidal harmonic analysis including error estimates in MATLAB using T_TIDE, *Comput. Geosci.*, *28*, 929–937.

Pietrafesa, L. J., and G. S. Janowitz (1980), Lack of evidence of southerly propagating continental shelf waves in Onslow Bay, N. C., *Geophys. Res. Lett.*, *7*, 113–116.

Pietrafesa, L. J., J. O. Blanton, J. D. Wang, V. Kourafalou, T. N. Lee, and K. A. Bush (1985), The tidal regime in the South Atlantic Bight, in *Oceanography of the Southeastern U. S. Continental Shelf*, *Coastal Estuarine Sci.*, vol. 2, edited by L. P. Atkinson, D. W. Menzel, and K. A. Bush, pp. 63–76, AGU, Washington, D. C.

Rabinovich, A. B., and R. E. Thomson (2001), Evidence of diurnal shelf waves in satellite-tracked drifter trajectories off the Kuril Islands, *J. Phys. Oceanogr.*, *31*, 2650–2668.

Savidge, D. K. (2002), Wintertime shoreward near-surface currents south of Cape Hatteras, *J. Geophys. Res.*, *107*(C11), 3205, doi:10.1029/2001JC001193.

Savidge, D. K. (2004), Gulf stream meander propagation past Cape Hatteras, *J. Phys. Oceanogr.*, *34*, 2073–2085.

Savidge, D. K., and J. A. Austin (2007), The Hatteras Front: August 2004 velocity and density structure, *J. Geophys. Res.*, *112*, C07006, doi:10.1029/2006JC003933.

Savidge, D. K., and J. M. Bane (2001), Wind and Gulf Stream influences on alongshelf transport and off-shelf export at Cape Hatteras, North Carolina, *J. Geophys. Res.*, *106*, 11,505–11,527.

Schwing, F. B., L.-Y. Oey, and J. O. Blanton (1988), Evidence for nonlocal forcing along the southeastern United States during a transitional wind regime, *J. Geophys. Res.*, *93*, 8221–8228.

Soulsby, R. L. (1990), Tidal-current boundary layers, in *The Sea*, *Ocean Eng. Sci. Ser.*, vol. 9, edited by B. Mehaugte and D. Hanes, pp. 523–566, Harvard Univ. Press, Cambridge, Mass.

Ullman, D. S., and P. C. Cornillon (1999), Satellite-derived sea surface temperature fronts on the continental shelf off the northeast U. S. coast, *J. Geophys. Res.*, *104*, 23,459–23,478.

Verity, P. G., J. Bauer, C. N. Flagg, D. DeMaster, and D. Repeta (2002), The ocean margins program: An interdisciplinary study of carbon sources, transformations, and sinks in a temperate continental margin system, *Deep Sea Res., Part II*, *49*, 4273–4295.

Wang, D.-P. (1979), Low frequency sea level variability on the Middle Atlantic Bight, *J. Mar. Res.*, *37*, 683–697.

C. R. Edwards, Department of Marine Sciences, University of North Carolina, 340 Chapman Hall, CB 3300, Chapel Hill, NC 27599, USA.

M. Santana, Center for Coastal Physical Oceanography, Old Dominion University, Crittenton Hall, Norfolk, VA 23529, USA.

D. K. Savidge, Skidaway Institute of Oceanography, 10 Ocean Science Circle, Savannah, GA 31411, USA. (dana.savidge@skio.usg.edu)